Nanoscale Solutions for Fungal Crop Diseases: Efficacy of Yttrium-Doped Barium Hexaferrites

Tamnna Kumari [a,b*], Indu Sharma [a,b] ,Neha Thakur[a,b] ,Indu Bhardwaj[c]

[a]Department of Physics, Career Point University Hamirpur, Himachal Pradesh, 176041, India
[b]Center for Green Energy Research, Career Point University Hamirpur, Himachal Pradesh, 176041, India
[c]Department of Microbiology, Career Point University, Hamirpur, Himachal Pradesh, 174061,India
***Corresponding author. Email:** tamannadhiman99@gmail.com*

Abstract
The impeding of pathogenic bacteria towards various treatment methods is flourishing concern in different areas including agriculture industry. The present work reports to study of antifungal properties of yttrium doped M-type Ba hexagonal ferrites. Samples of Barium Hexaferrite doped with yttrium.i.e. $BaFe_{12-x}Y_xO_{19}$ with (x = 0.0, 0.2) were synthesized by the citrate precursor technique. Nanoferrites were dispersed with buffer solution for the preparation of different concentration. 50% and 100%. Colletotrichum truncatum (MTCC 2110) and Rhizoctonia solani(MTCC 9666) were used as fungal strains. To ascertain the minimum inhibitory concentration, researchers employed the agar well diffusion technique. Yttrium doped barium hexa ferrites were determined to be an effective antifungal nanomaterial. This study suggested that yttrium doped Barium hexaferrites are assuring high efficacy antifungal nanomaterial. Transmission electron microscopy (TEM) used for structural and morphological studies.

Keywords: M-types barium hexaferrites; rhizoctonia solani; Colletotrichum truncatum

1. INTRODUCTION

One of the most common and varied groups of unusual organisms is the fungus. Several fungus species are plant pathogens. Fungal pathogens have been regularly identified and described as developing and reemergin[1]. Originally included in the Kingdom Plantae, fungi were separated out into their own kingdom in 1969 and given their own kingdom, Kingdom Fungi, which includes a variety of groupings with distinct morphologies, including multicellular creatures and unicellular yeasts[2]. Utilizing nanoparticles (NPs) as an antifungal treatment is one practical arrangement. Albeit this area of nanotechnology is the subject of a few investigations, little is had some significant awareness of the components of activity basic the utilization of NPs as an antifungal[3]. Maize is a wonder crop that will usher in the yellow revolution. With the largest production potential of any cereal, being the "Queen of Cereals," it may be extremely helpful in guaranteeing food and nutritional security for both India and the rest of the globe. Banded leaf and sheath blight, a disease caused by *R. solani*, is attributed to one of the most ubiquitous, damaging, and flexible pathogens found across numerous regions

of the world. This microorganism has the potential to affect various plant hosts, including Zea mays, causing deterioration in their seeds[4]. *Rhizoctonia solani* causes a large number of plant sicknesses over a more noteworthy piece of the world and under different natural circumstances, more noteworthy than some other plant harmful microbes, instance, mung bean, damping down during the seedling and podding stages, root decay, and seed rot[5]. Plant pathogens that are well-known in tropical and subtropial regions are *Colletotrichum species*. Even scientists that specialize in the taxonomy and nomenclature of *Colletotrichum species* find it confusing[6]. Grown for its flavor, nutritional content, and color, it is referred to as a wonder spice[7]. With almost 400 types grown globally, In global vegetable rankings, this crop holds the fourth position of significance, while it claims the premier spot within the Asian continent. India is the world's largest importer, exporter, and producer of chiles[8]. Although chili is produced year-round in India, the average output is still quite modest. Chilli production faces a serious challenge from *Colletotrichum truncatum*, which causes anthracnose disease[9]. One common illness affecting chilies (Capsicum) is anthracnose, which is brought on by a group of *Colletotrichum species* [10]. Antifungal properties, with specific types causing significant inhibition of mycelial growth, disease occurrence, and lesion length in rice seedlings[11]. Similarly, bacterial strains, like Bacillus subtilis, have demonstrated clear antagonism against *R. solani*, making them promising candidates for biocontrol applications[12]. The compound CF66I has exhibited broad-spectrum antifungal activity against *R. solani*, and has been found to cause morphological changes in fungal cells[13]. Additionally, virtual screening has led to the identification of compounds, such as Hit8, that inhibit *R. solani* DHFR and display antifungal properties[14]. Investigations have examined the potential of microalgal extracts to inhibit *R. solani* growth, with specific strains demonstrating promising inhibitory effects. The use of polygalacturonase-inhibiting proteins (PGIPs) from beans has also been explored as a means of inhibiting *R. solani* in canola, and transgenic overexpression has shown promise[15]. Approximately 189 varieties constitute the genus *Colletotrichum*, which is divided into 11 associations: *gigasporum, gloeosporioides, boninense, truncatum, orbiculare, graminicola, spaethianum, destructivum, acutatum, dematium,* and *caudatum*. These fungi are responsible for causing anthracnose in a wide variety of plant kinds, especially crops that are important to agriculture and the economy[16]. Many plant diseases that affect veggies, beans, grains, and tropical and non-tropical crops can be identified in the family *Colletotrichum* (Sordariomycetes, Ascomycota)[17]. *Colletotrichum truncatum*, a fungal species, predominantly affects soybeans, lentils, and papayas. The *Colletotrichum genus* is responsible for anthracnose, a widespread disease impacting legume crops globally. Approximately 600 plant varieties within the *Colletotrichum* classification can significantly damage various crops, exhibiting characteristic indicators such as depressed necrotic lesions, generally termed anthracnose. In sword beans, researchers have identified *Colletotrichum capsica* in China and *Colletotrichum lindemuthianum* in India. Anthracnose represents a significant threat to sword bean cultivation[18]. Characterized by its high coercivity (Hc), barium M-type hexaferrite is commonly classified as a hard-ferromagnetic material. The structure of barium hexaferrite (BHF), an M-type hexagonal ferrite, exhibits centrosymmetry along the c-axis of rapid magnetization. It comprises four distinct sections: S, S*, R, and R*. This hexaferrite, which belongs to the P63/mmc space group, features iron ions distributed across various sites: three octahedral (12k, 4f2, and 2a), one tetrahedral (4f1), and

one bipyramidal (2b). The 4f1 and 4f2 positions contain four Fe3+ ions with upward spins, while eight Fe3+ ions with upward spins are found in each of the five sub-lattices (12k, 2a, and 2b). Consequently, the four-remaining upward-rotating positions yield a total magnetic moment of 20 μB[19]. The characteristics of barium hexaferrites, also referred to as hard magnetic materials, are high magnetism, Curie temperature, low prices, affordability, and degrading resistance[20]. Despite extensive research on the magnetic properties of $BaY_xFe_{12-x}O_{19}$, there remains a significant knowledge gap regarding its potential application as an antifungal agent. While the magnetic characteristics of this material have been thoroughly documented, its efficacy against fungal pathogens has yet to be investigated. Specifically, the antifungal properties of $BaY_xFe_{12-x}O_{19}$with yttrium doping at x values of 0.0 and 0.2 have not been examined in relation to *Rhizoctonia solani (MTCC 9666)* and *Colletotrichum truncatum (MTCC 2110).* Furthermore, the use of the agar well diffusion technique to assess the antifungal efficacy of the synthesized hard ferrite materials represents a novel approach in this field of study. This investigation aimed to address these knowledge gaps and potentially elucidate new applications of BaYxFe12-xO19 in inhibiting fungal growth.

2. MATERIALS AND METHOD

2.1 MATERIALS

Strains of two plant pathogens *Colletotrichum truncatu*m (MTCC 2110) and *Rhizoctonia solani f sp sasakaii* (MTCC 9666) were used for antifungal activity. Both strains were purchased from Institute of Microbial technology Chandigarh, India.

2.2 METHOD

2.2.1 TEM (Transmission Electron Microscope)

The surface morphology of the particles was examined by Transmission Electron Microscopy (TEM). TEM images were obtained using a High-Resolution Transmission Electron Microscope [HRTEM] at the IIT Roorkee. ImageJ software was used to analyze the micrographs.

2.2.2 Antifungal activity of ferrite Nanoparticles against *Rhizoctonia solani* and *Colletotrichum truncatum* via Agar well plate diffusion Method.

The agar well diffusion method was employed to evaluate the antifungal efficacy of the M-type $BaFe_{12-x}Y_xO_{19}$ (x = 0.0 and 0.2) nanoparticles. Two plant pathogens, *Colletotrichum truncatum* (MTCC 2110) and *Rhizoctonia solani f. sp. sasakaii* (MTCC 9666), were selected for investigation. Fungal cultures were prepared and maintained according to standard microbiological protocols. Potato Dextrose Agar (PDA) medium was prepared, sterilized, and dispensed into Petri dishes. Following solidification, 100 μL of the fungal culture suspension was uniformly distributed across the agar surface using a sterile spatula to ensure homogeneous growth [21]. Three wells, each 6 mm in diameter, were created in the inoculated PDA medium

using the reverse end of a sterile micropipette tip. M-type $BaFe_{12-x}Y_xO_{19}$ nanoparticles (x = 0.0 and 0.2) were prepared at two specific concentrations: 50% and 100%. The nanoparticles, produced in ethanol using a volume-to-volume ratio, were subsequently deposited into cavities previously created on the plates. The inoculated petri dishes were incubated at 37°C for 24 hours[22]. Incubation, the dishes were examined for zones of inhibition surrounding the wells, and the diameters of these zones were measured in millimeters. The antifungal assay was conducted in triplicate to ensure reproducibility and statistical significance.

3. RESULT AND DISCUSSION

3.1 Synthesis and Chemical characterization of material[23].

TEM Analysis

TEM analysis of $BaFe_{12-x}Y_xO_{19}$(x=0.1) ferrite nanoparticles provided comprehensive insights into their structural, morphological, and size characteristics. The TEM images revealed that the nanoparticles exhibited a nearly hexagonal morphology, which was consistent with the expected crystal structure of M-type barium hexaferrite. The particles demonstrated slight agglomeration, which is typically attributed to strong magnetic interactions and van der Waals forces between the particles as shown in **Figure(i)**. Observations revealed particles of varying dimensions and configurations. The particle size distribution, derived from TEM micrographs, showed an average particle size of 15 ± 0.37 nm, confirming the successful synthesis of nanoparticles within the desired nanoscale range. This nanoscale dimension is crucial for the unique properties of ferrite nanoparticles, including enhanced magnetic and electrical characteristics. High-resolution TEM (HRTEM) images further emphasized the crystalline nature of the nanoparticles, showcasing well-defined lattice fringes that correspond to the interplanar spacings specific to the crystal structure. These lattice fringes confirm the crystallinity and structural integrity of the synthesized material. The findings from the TEM analysis align with the results of XRD, which also indicated phase purity and crystallinity, thereby reinforcing the reliability of the synthesis method employed. The nanoscale size, coupled with the crystalline structure of $BaFe_{12-x}Y_xO_{19}$(x=0.1) nanoparticles, plays a pivotal role in their potential applications. These properties make them ideal candidates for various technological applications, particularly in magnetic storage devices, catalysts, and electronic components. The TEM study not only verifies the structural and morphological attributes but also highlights the potential of $BaFe_{12-x}Y_xO_{19}$(x=0.1) nanoparticles in cutting-edge industrial and technological advancements.

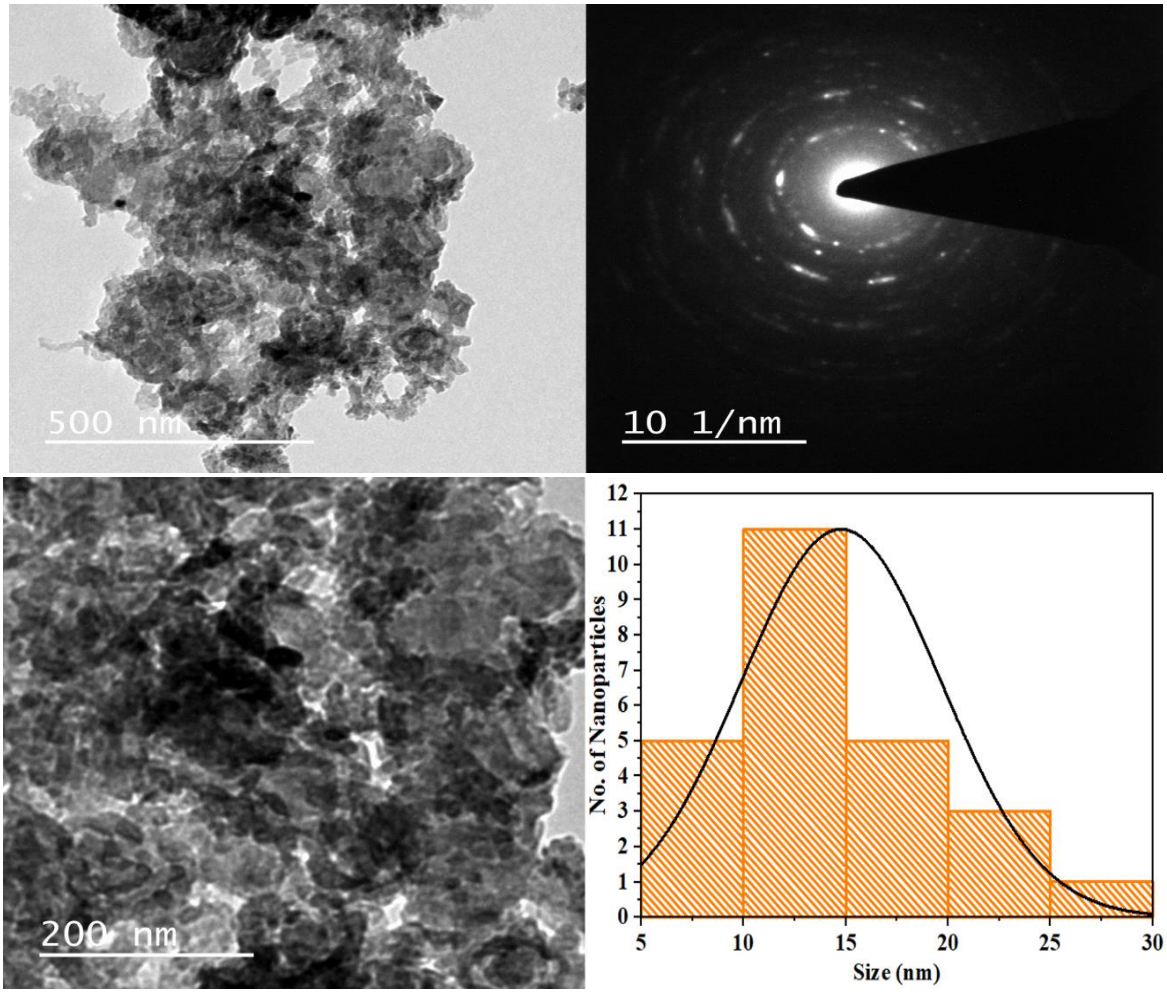

Figure (i) TEM analysis of $BaFe_{12-x}Y_xO_{19}$(x=0.1) ferrite nanoparticles

3.2 Antifungal Activity

3.2.1 Cultivation of culture

Rhizoctonia solani and *Colletotrichum truncatum*, obtained from the Microbial Type Culture Collection (MTCC), were cultivated on Potato Dextrose Agar (PDA). PDA medium was prepared using commercially available powder and sterilized by autoclaving at 121°C for 15-20 minutes before being dispensed into sterile Petri dishes. Pure cultures of *R. solani* and *C. truncatum* were obtained from MTCC following the manufacturer's instructions for revival and handling. Using a sterile inoculation loop, a small quantity of fungal mycelia or spores was transferred from the MTCC culture to the center of the PDA plate, which was then sealed with Parafilm to prevent contamination. The plates were incubated at 25-28°C for *R. solani* and at 22-25°C for *C. truncatum* for 5-7 days or until sufficient growth was observed. The cultivation of both fungal cultures is illustrated in **Figure (ii) (a,b).** The cultures were regularly monitored for contamination and subculture on fresh PDA plates every 2-4 weeks to maintain viability. For short-term storage, cultures were maintained at 4°C.

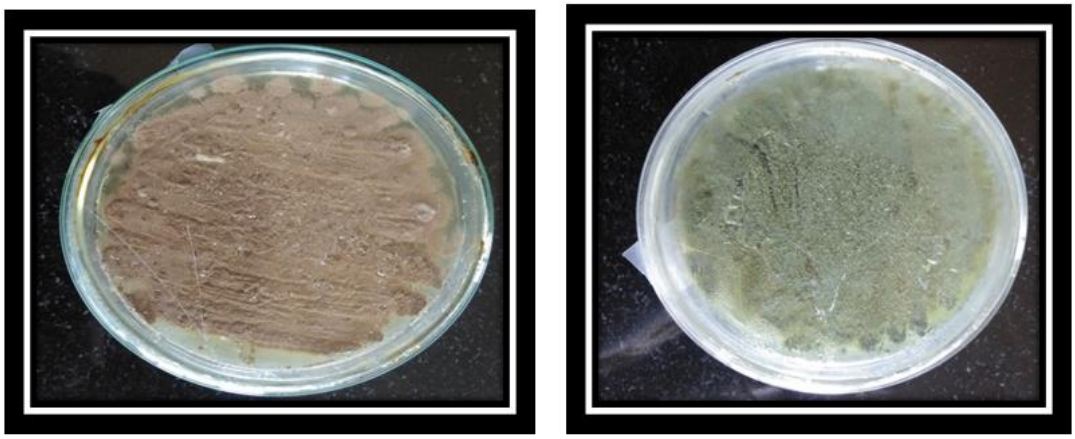

Figure (ii) (a,b) shows the cultivation of both the fungus culture.

3.2.2 Antifungal Assay

Figure (iii) (a,b) illustrates the antifungal activity of yttrium-substituted barium hexaferrite nanoparticles examined against *Rhizoctonia solani* for compositions x = 0.0 and 0.2. In **Figure (iii) (a),** it is evident that x = 0.0 demonstrates antifungal activity against *Rhizoctonia solani* fungus only at 100% concentration, with no observable effects at 50% concentration. Conversely, **Figure (iii)(b**) shows the inhibition zone against *Colletotrichum truncatum* at both 50% and 100% concentrations. The measured inhibition zones for both samples are listed in Table **(i)**.

Figure (iv) presents a bar graph representation of *Rhizoctonia solani* fungus for pure and yttrium-substituted barium M-type hexaferrites for the samples with x = 0.0 and 0.2 nanoparticles. The bar graph illustrates the results for both the prepared samples at 50% and 100% concentrations.

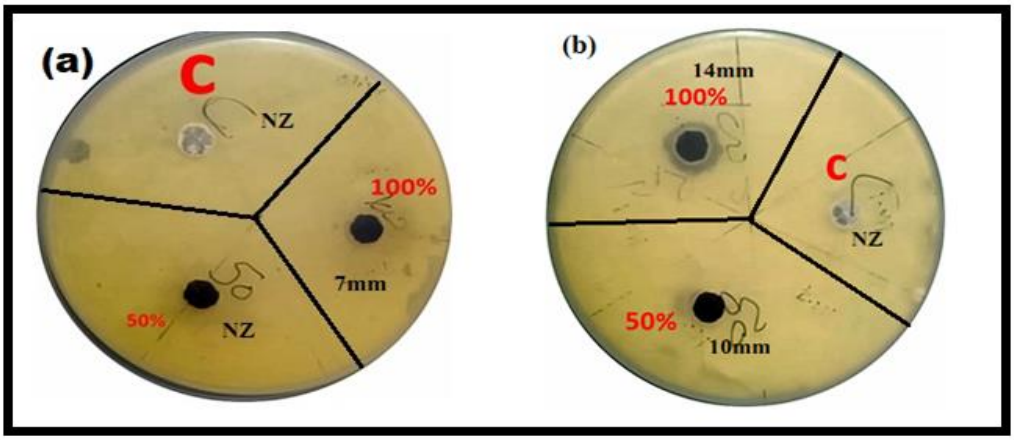

Figure (iii) (a,b) Illustrates the zones again for *Rhizoctonia solani* fungus for $BaFe_{12-x}Y_xO_{19}$(x=0.0, x=0.2) nanoparticles.

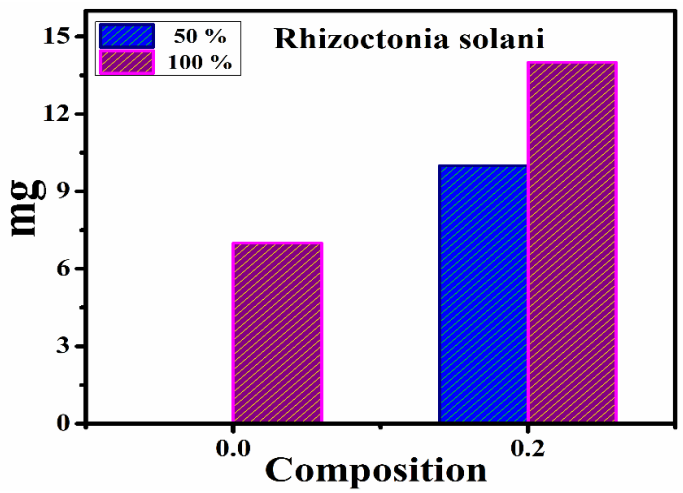

Figure (iv) graph depicts the effectiveness of barium hexaferrites, both pure and yttrium-doped, when tested against *Rhizoctonia solani*.

Figure (v) (a) and (b) present the results against the *Colletotrichum truncatum* fungus for the pure and yttrium-substituted barium hexaferrites for the prepared samples with x = 0.0, 0.2 nanoparticles. The figure demonstrates that both the synthesized samples exhibited antifungal activity against this organism. For the pure composition, inhibition zones of 7 and 13 mm were observed for the 50% and 100% concentrations, respectively. For x = 0.2 concentration, inhibition zones of 11 mm and 16 mm were observed for 50% and 100% concentrations, respectively, indicating that higher concentrations yield more pronounced antifungal effects. **Figure (vi)** provides a graphical representation of the antifungal activity of $BaY_xFe_{12-x}O_{19}$ (x = 0.0, x = 0.2) nanoparticles against *Colletotrichum truncatum*. This graphical representation illustrates the antifungal efficacy of both the samples at 50% and 100% concentrations.

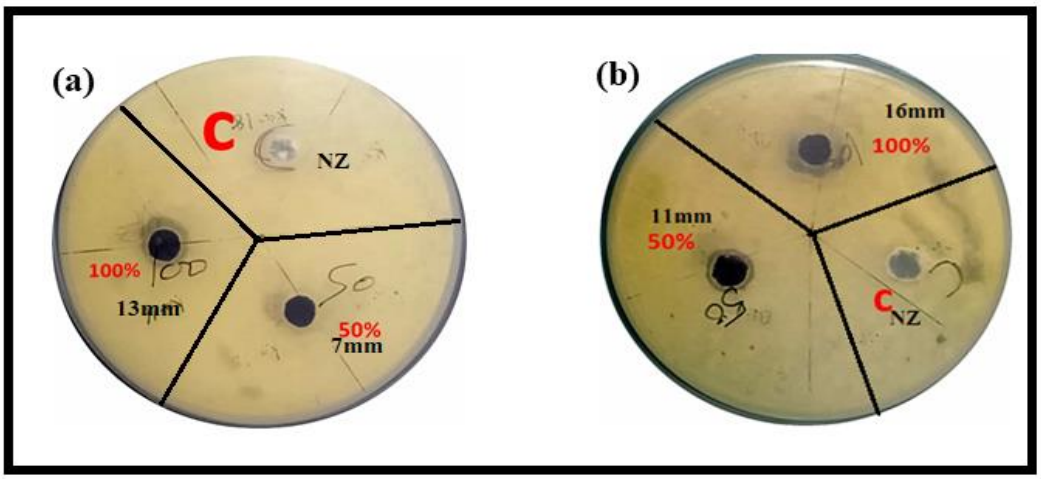

Figure (v) (a,b) illustrates the results obtained for pristine and yttrium-substituted barium hexaferrite nanoparticles at x=0.0 and 0.2, as demonstrated by the *Colletotrichum truncatum* fungus.

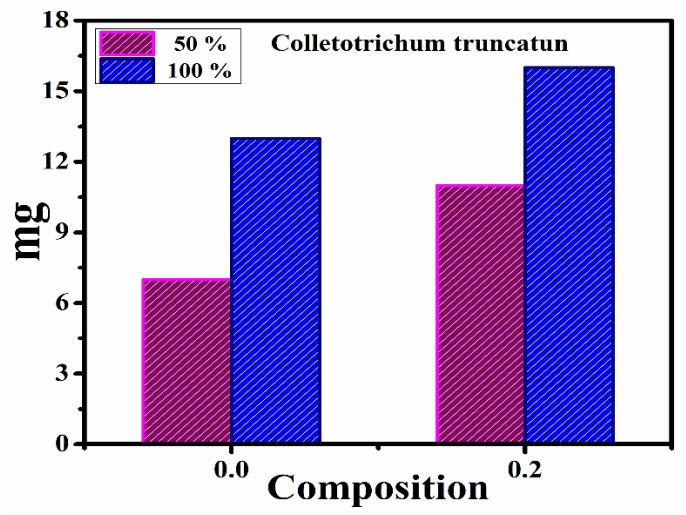

Figure (vi) shows the bar graph of both the sample of barium hexaferrites nanoparticles against *Colletotrichum truncatum*.

Table(i) Antifungal activity of $BaFe_{12-x}Y_xO_{19}$against *Rhizoctonia solani* and *Collectotrichum truncatum* for x=0.0 and x=0.2.

Sr.No.	Composition	Concentration (x)	Zone in diameter (mm) *Rhizoctonia solani*	Zone in diameter (mm) Collectotrichum Truncatum
1.	Control	------	-----	------
2.	x=0.0	50 %	None	10±0.2mm
		100 %	7±0.2 mm	14±0.1 mm
3.	x=0.2	50 %	10±0.1 mm	11±0.3 mm
		100 %	14±0.2 mm	16±0.1 mm

The antifungal activity of the undoped (x=0.0) and doped (x=0.2) compositions was tested against *Rhizoctonia solani* and *Colletotrichum truncatum* at 50% and 100% concentrations. The results showed that doping and higher concentrations significantly enhanced antifungal efficacy. For R. solani, the undoped composition was minimally effective, showing no inhibition at 50%, and moderate inhibition (7 mm) at 100%. However, the doped composition displayed improved activity, with 10 mm inhibition at 50% and 14 mm at 100%. This indicated the substantial impact of doping on the antifungal properties of *R. solani*. *C. truncatum* was more susceptible overall. The undoped composition showed 10 mm inhibition at 50% and 14 mm at 100%, whereas the doped composition achieved 11 mm at 50% and 16 mm at 100%. These findings highlight that doping enhances antifungal activity for both fungi, with the doped composition at 100% doping being the most effective. The greater inhibition observed in *C.*

truncatum suggests that differences in cell wall structures or metabolic processes affect their response to antifungal agents.

The antifungal activity of Y-doped barium hexaferrite nanoparticles against *R. solani* and *C. truncatum* is due to several mechanisms. These nanoparticles generate Reactive Oxygen Species (ROS) that damage fungal cell membranes, proteins, and DNA. They also disrupt membrane integrity through direct interactions, causing cell death. The release of yttrium ions may interfere with fungal cellular processes. Charged nanoparticles engage in electrostatic interactions with fungal cell surfaces, affecting membrane potential and cellular functions. Additionally, these nanoparticles inhibit key fungal enzymes and alter gene expression, impacting growth and survival. Direct contact with fungal cells can cause physical damage, enhancing their antifungal effects. Consequently, the development of effective alternatives to chemical fungicides remains a significant challenge in the field [24]. These outcomes show that synthesized nanoparticles can track down application as anti-microbials against these organisms.

CONCLUSION

This study highlighted the significant influence of doping and concentration on the antifungal properties of the tested compositions against *Rhizoctonia solani* and *Colletotrichum truncatum*. Doping consistently improved the antifungal efficacy for both fungal species, with the doped composition (x=0.2) outperforming the undoped composition (x=0.0) at both 50% and 100% concentrations. The 100% concentration of the doped composition was the most effective, achieving the maximum inhibition zones for both fungi. *C. truncatum* showed higher susceptibility than *R. solani*, suggesting differences in their cellular structures or metabolic processes. These results indicate that doping is a viable strategy for enhancing antifungal properties and optimizing the \composition and concentration for effective fungal control. Further research into the mechanisms underlying the enhanced antifungal activity of doped compositions could aid the development of more potent and targeted antifungal agents. TEM analysis revealed nearly hexagonal $BaFe_{12}0_{19}$ ferrite nanoparticles with an average size of 15 ± 0.37 nm and high crystallinity. This study not only verifies the structural morphological and antimicrobial attributes but also underscores the potential of these nanoparticles in advancing various fields.

Acknowledgement

Author Indu Sharma is also thankful to H. P. Council for Science, Technology & Environment for granting project HIMCOSTE (R & D)/2023–24–6 (4).

Author Contributions

This research represents a collaborative effort with equal contributions from all authors. The study's conceptualization and editorial supervision were undertaken by Indu Sharma. Tamnna Kumari was responsible for the preparation and organization of the initial manuscript draft. Neha Thakur and Indu Bhardwaj: Methodology. The final version of the manuscript emerged through the collective input of all authors, each of whom has given their approval to the definitive document.

Data availability

The dataset underlying the conclusions drawn in this investigation is accessible through direct correspondence with the study's corresponding author.

Rival interests

The authors declare no conflict of interest.

REFRENCES:

1. Pereira, L., et al., Synthesis, characterization and antifungal activity of chemically and fungal-produced silver nanoparticles against Trichophyton rubrum. Journal of applied microbiology, 2014. **117**(6): p. 1601-1613.

2. Whittaker, R.H., New Concepts of Kingdoms of Organisms: Evolutionary relations are better represented by new classifications than by the traditional two kingdoms. Science, 1969. **163**(3863): p. 150-160.

3. Slavin, Y.N. and H. Bach, Mechanisms of antifungal properties of metal nanoparticles. Nanomaterials, 2022. **12**(24): p. 4470.

4. Singh, S., et al., Rhizoctonia solani f. sp. sasakii inciting banded leaf and sheath blight of maize and their management: an overview. International Journal of Current Microbiology and Applied Sciences, 2019. **8**(07): p. 2858-2866.

5. SINGH, D., et al., Diversified products of sugarcane juice: Helpful in fetching higher price in the market. THE JOURNAL OF RURAL AND AGRICULURAL RESEARCH, 2009. **9**(2): p. 18-20.

6. Hyde, K., et al., Colletotrichum—names in current use. Fungal Diversity, 2009. **39**(1): p. 147-182.

7. Bosland, P.W. and E.J. Votava, Peppers: vegetable and spice capsicums. 2012: Cabi.

8. Singhal, V., Indian Economic Data Research Centre. New Delhi, 1999: p. 60-71.

9. Chethana, C., P. Chowdappa, and K. Pavani, Colletotrichum truncatum and C. fructicola causing anthracnose on chilli in Karnataka state of India. Indian Phytopathology, 2015. **68**(1): p. 270-278.

10. Than, P., et al., Characterization and pathogenicity of Colletotrichum species associated with anthracnose on chilli (Capsicum spp.) in Thailand. Plant pathology, 2008. **57**(3): p. 562-572.

11. Liu, H., et al., Antifungal effect and mechanism of chitosan against the rice sheath blight pathogen, Rhizoctonia solani. Biotechnology letters, 2012. **34**: p. 2291-2298.

12. Elkahoui, S., et al., Evaluation of antifungal activity from Bacillus strains against Rhizoctonia solani. African Journal of Biotechnology, 2012. **11**(18): p. 4196-4201.

13. Li, X., C.S. Quan, and S.D. Fan, Antifungal activity of a novel compound from Burkholderia cepacia against plant pathogenic fungi. Letters in applied microbiology, 2007. **45**(5): p. 508-514.

14. Feng, R., et al., Discovery of novel Rhizoctonia solani DHFR inhibitors as fungicides using virtual screening. Journal of Agricultural and Food Chemistry, 2023. **71**(49): p. 19385-19395.

15. Akhgari, A.B., M. Motallebi, and M.R. Zamani, Bean polygalacturonase-inhibiting protein expressed in transgenic Brassica napus inhibits polygalacturonase from its fungal pathogen Rhizoctonia solani. Plant Prot. Sci, 2012. **48**: p. 1-9.

16. Cortaga, C.Q., et al., Mutations associated with fungicide resistance in Colletotrichum species: A review. Phytoparasitica, 2023. **51**(3): p. 569-592.

17. Guevara-Suarez, M., et al., Colletotrichum species complexes associated with crops in Northern South America: a review. Agronomy, 2022. **12**(3): p. 548.

18. Shi, M., et al., Colletotrichum truncatum—A new etiological anthracnose agent of sword bean (Canavalia gladiata) in Southwestern China. Pathogens, 2022. **11**(12): p. 1463.

19. Sharma, I., et al., Enhanced photocatalytic and antimicrobial properties of nickel-doped barium M-type hexaferrites synthesized via citrate sol-gel method. Inorganic Chemistry Communications, 2024. **169**: p. 113116.

20. Thakur, N., et al., Improvement in the structural, magnetic and electromagnetic behaviour of barium hexaferrites with yttrium doping for EMI shielding. Journal of Alloys and Compounds, 2024. **976**: p. 173042.

21. Martinson, K.D., et al., Synthesis, Structure, and Antimicrobial Performance of NixZn1− xFe2O4 (x= 0, 0.3, 0.7, 1.0) Magnetic Powders toward E. coli, B. cereus, S. citreus, and C. tropicalis. Water, 2022. **14**(3): p. 454.

22. Ishaq, K., et al., Characterization and antibacterial activity of nickel ferrite doped α-alumina nanoparticle. Engineering Science and Technology, an International Journal, 2017. **20**(2): p. 563-569.

23. Sharma, I., et al., Citrate precursor route for Y3+ substituted M-type Ba-hexaferrite: synthesis, the effect of doping on structural, optical, magnetic and anti-bacterial properties. Materials Chemistry and Physics, 2023. **302**: p. 127664.

24. Zhang, J., et al., Antifungal activity and mechanism of palladium-modified nitrogen-doped titanium oxide photocatalyst on agricultural pathogenic fungi Fusarium graminearum. ACS applied materials & interfaces, 2013. **5**(21): p. 10953-10959.